# Chapter 4

# Spin-S Ising ferromagnet driven by Propagating and Standing magnetic field wave.

## 4.1 Introduction:

We have seen that many studies were done to reveal the characteristic behaviors of different nonequilibrium driven ferromagnets. Those studies were carried out on specific types (having a particular spin value) of ferromagnetic systems [[1]-[14]]. In the previous chapters, I have discussed about the nonequilibrium phase transition in specific types of ferromagnet; viz. spin-$\frac{1}{2}$ (Ising) [15, 16] or spin-1 (Blume-Capel) [17] ferromagnet driven by magnetic waves. In those studies, I showed how the ferromagnetic spins response to different kind of magnetic waves.

However, this would be interesting and relevant to know the dynamical behavior of a general spin-$S$ ferromagnetic system having $(2S + 1)$ number of spin states or spin degeneracies. Is there any universal characteristic for dynamical phase transition under time dependent driving field for such system of general spin-$S$ ferromagnet? This chapter is devoted to this specific question. I intend to elaborate here the dynamical response of $S$- spin Ising ferromagnet to the plane propagating wave, standing magnetic field wave and uniformly oscillating field all having a constant frequency. The studies were made separately in two dimensions by extensive Monte Carlo simulation with Metropolis Single spin flip algorithm and are presented here in details in the following sections. These studies were published in the journal, whose reference is given as follows:
**Ajay Halder** and **Muktish Acharyya** *Commun. Theor. Phys.* **68**(2017)600.

## 4.2 Magnetic waves through spin-$S$ Ising ferromagnet:

The dynamical response of a 2-state (spin$\frac{1}{2}$) Ising ferromagnet driven by magnetic waves has been discussed in *section 2.2*. When magnetic waves are moving through an Ising ferromagnet the ferromagnetic spins respond to the spatio-temporal variation (magnetic perturbation) of the magnetic field. This perturbation excites the spins to transit between their available states by thermal fluctuation. The dynamics of spins not only depends on the nature of the magnetic waves but also upon the number $(n = 2S + 1)$ of available states of a general spin-$S$ Ising ferromagnet. Thus, the dynamical patterns of the spin states and the dynamical transition temperature for transition between symmetric phase and symmetry- broken phase vary with the value $S$.

### 4.2.1 Response to propagating magnetic wave:

The time dependent Hamiltonian of a two dimensional Ising ferromagnet, having $(2S+1)$ numbers of spin states and uniform nearest neighbor interaction, in presence of a magnetic field wave (having spatio-temporal variation) can be expressed as-

$$H(t) = -J\Sigma\Sigma' s^z(x,y,t)s^z(x',y',t) - \Sigma h^z(x,y,t)s^z(x,y,t), \tag{4.1}$$

where, $s^z(x,y,t)$ represents the $z$ component of *unit* spin. The general spin ($S$) is normalized to unity; i.e. the magnitude of each spin is unity. Depending on the value of $S$, the $z$-components of unit spin $s^z$ takes any of the $(2S+1)$ values of spin state, viz, $+1,\ +\frac{|(S-1)|}{|S|},\ ...,\ -1$. The first and the second terms represent respectively the spin-spin cooperative energy and the spin-magnetic field interaction energy. "$\Sigma'$" indicates that summation is extended upto nearest neighbors only. The magnetic field $h^z(x,y,t)$ at site $(x,y)$ at time $t$, has the following form of propagating wave:

$$h^z(x,y,t) = h_0 cos(2\pi ft - 2\pi\frac{x}{\lambda}).$$

Here, $h_0, f$ and $\lambda$ represent respectively *the field amplitude, the frequency of magnetic field oscillation and the wavelength* of the propagating magnetic wave.The cooperative interaction strength $J$ is considered to be uniform throughout the system like the cases mentioned earlier.

#### Monte-Carlo simulation:

Again, we choose a simple model here. A square lattice of dimension $L \times L$ is taken over which the unit spins are arranged. The dynamics of such spins are imposed by *Monte-Carlo* method [18]. To see the bulk behavior of a $2D$ Ising ferromagnet, we preserve the translational invariance in the lattice by applying periodic boundary conditions in both the $x$ and $y$ directions of the square lattice. The initial configuration of spins in the lattice corresponds to the high temperature random phase where all the $(2S+1)$ values of spin states $(+1,\ \ +\frac{|(S-1)|}{|S|},\ ...,\ \ -1)$ are uniformly distributed over all the lattice sites. At any temperature, the ferromagnetic spins respond to the propagating magnetic wave depending on the values of the parameters such as cooperative interaction strength $J$, the instantaneous value of the magnetic field $h(t)$ and the value of general spin $S$. These responses of individual ferromagnetic spins manifest collectively, in the form of dynamical patterns in the spin-lattice. The system is cooled down slowly by decreasing the temperature in small values and every dynamical steady state is thus achieved. Steady state behavior at any particular temperature is observed by keeping the ferromagnet at that constant thermal bath for a sufficiently long time. During this time the spins are updated at the metropolis rate given by *equation 2.3* :

$$W(s_i^z \rightarrow s_f^z) = Min[exp(-\Delta E/kT), 1].$$

Here $s_i^z$ and $s_f^z$ represent the initial and final values of any spin state at a site $(x, y)$, before and after updating, respectively. $\Delta E$ represents the change in energy due to the change in $s^z$ from initial state to final state; $k$ is the Boltzmann constant. The field amplitude $h_0$ is measured in the unit of $J$ whereas, the temperature $T$ is measured in the unit of $\frac{J}{k}$. The unit of time is *MCSS*, which is the time required to update an $L^2$ number of spins once in an $L \times L$ square lattice.

**Results:**

Monte-Carlo (MC) technique with parallel updating rule is used to simulate the dynamics of a general spin-$S$ Ising ferromagnet through which a linearly polarized propagating wave is passing. In steady state two different phases have been identified; namely: high temperature *symmetric* phase and low temperature *symmetry-broken* phase depending upon the temperature, magnetic field amplitude and the value of spin-$S$. In symmetric phase all the spin states corresponding to any $S$ value are symmetrically distributed over the lattice. At higher temperatures thermal fluctuations are larger, so the mutual interaction between the nearest neighbor spin states is insufficient to lock the spins at any particular state. These spins coherently follow the magnetic disturbance in the form of propagating wave, thus propagating bands of spins are observed within the lattice. Hence, this phase is also named the *propagating* phase. Again, it must be remembered that this propagating wave has no relation with that of the conventional spin wave in condensed matter physics. In propagating phase, spins are symmetrically distributed over a full wavelength of propagating wave. If the temperature of the $S$-spin Ising ferromagnet is now cooled down below a certain transition temperature, the thermal fluctuations get weaker. The propagating magnetic wave fails to break the mutual interaction between the unit spins. As a result most of the spins are aligned together along any particular direction and the spins are locked in either $+1$ or $-1$ values, i.e. spins states are asymmetrically distributed over the lattice. This phase is called the *pinned* phase. In propagating phase, the population of spin states other than $\pm 1$, is higher near the zero value of magnetic field. The reason is that at those points the influence of external magnetic field is minimum.

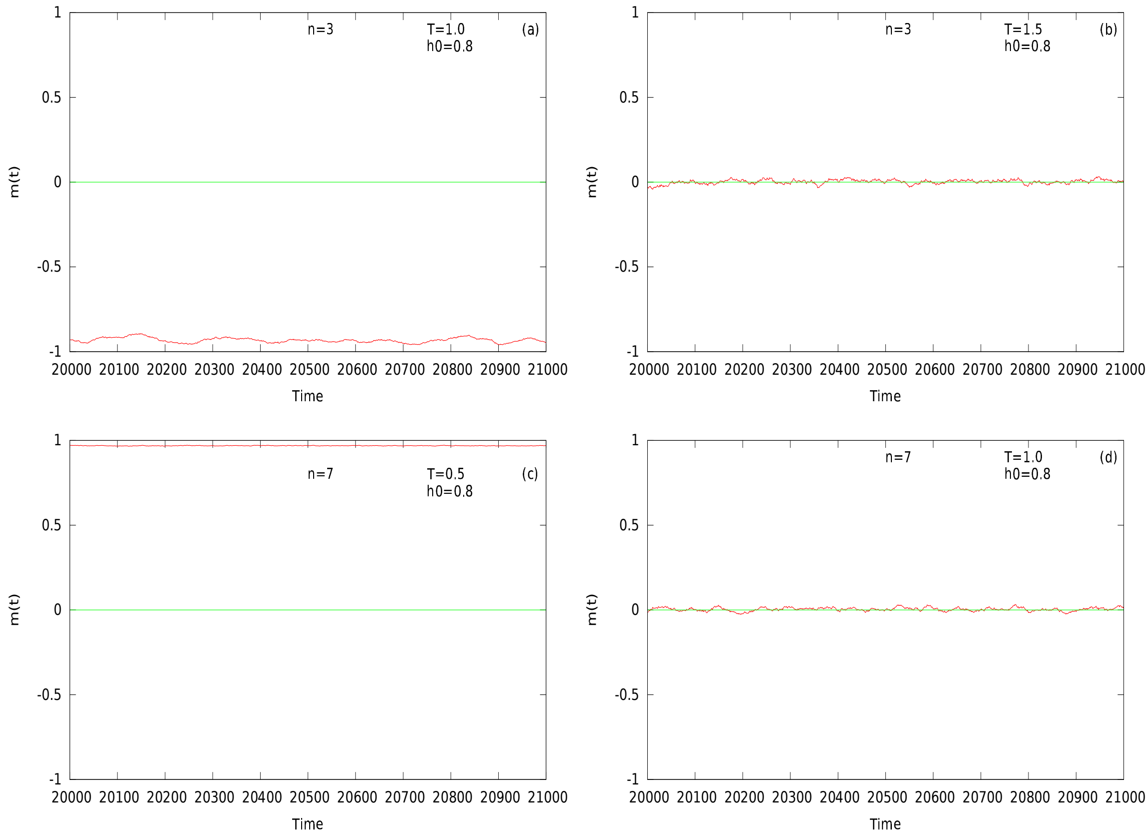


Figure 4.1: (Color online) Variation of magnetization with time at constant temperature ($T$) and field amplitude ($h_0$) for propagating wave. Figs. (**a**) & (**b**). represent *3-state* spin ($S = 1$) whereas figs. (**c**) & (**d**). represent *7-state* spin ($S = 3$). Frequency $f = 0.01$.

The order parameter for such a transition is defined, as usual, as the average magnetization per site over a full time period of magnetic field oscillation of propagating magnetic wave and is given by the equation : $Q = f \times \oint M(t)dt$, where $M(t) = \frac{1}{L^2}\sum_i s_i^z(x, y, t)$, is the magnetization per site at a particular time. At very high temperature the symmetric distribution of spin states gives rise to a very low value of order parameter. On the other hand, the asymmetric distribution of spin states below dynamic transition temperature gives rise to higher value of order parameter. The variation of order parameter with temperature is shown in *figure 4.2*(**a**).

The variation of magnetization with time in symmetric phase and symmetry-broken phase are shown in *figure 4.1* for two different values of $S$; viz. $S = 1$ and $S = 3$ respectively. In symmetric phase magnetization varies around zero value resulting in very low average whereas it varies around a nonzero value in symmetry-broken phase.

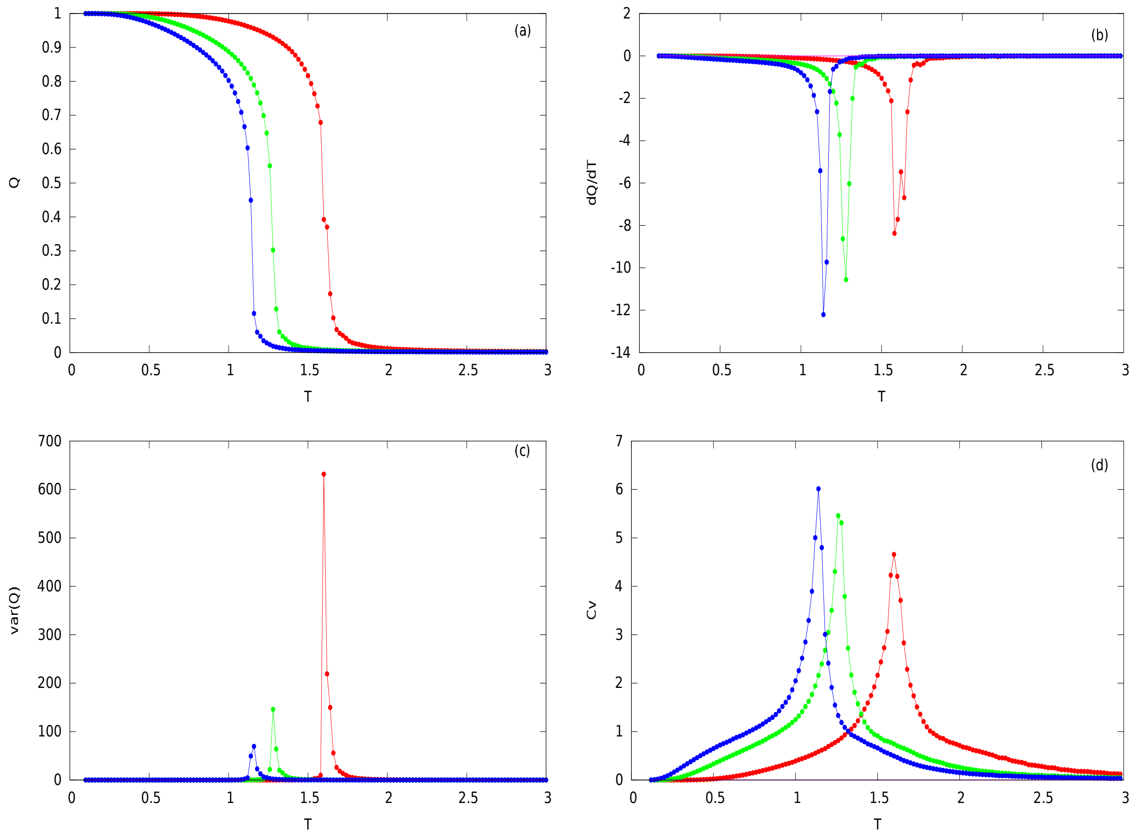


Figure 4.2: (Color online) Temperature variation of (**a**) $Q$, (**b**) $\frac{dQ}{dT}$, (**c**) $V$, (**d**) $C_v$ for *3-state* (red dot), *5-state* (green dot) and *7-state* (blue dot) spins for constant field amplitude ($h_0 = 0.2$) and frequency ($f = 0.01$) of propagating wave.

The variation of different dynamical quantities at steady state; such as: order parameter ($Q$), time derivative of the order parameter $\frac{dQ}{dT}$, variance of the order parameter ($V = L^2(\langle Q^2\rangle - \langle Q\rangle^2)$), and the dynamical heat capacity ($C_v = \frac{dE}{dT}$) with temperature for 3-state ($S = 1$), 5-state ($S = 2$) and 7-state ($S = 3$) spins respectively are shown in *figure 4.2*. These typical data are obtained from a $100 \times 100$ square Ising lattice. A propagating wave of wavelength $\lambda = 25\ lu$ and frequency $f = 0.01\ MCSS^{-1}$ is allowed to pass through the lattice. That is one complete cycle of magnetic oscillation takes a

100 MCSS time. To obtain each steady state value of these dynamical quantities, data (or values) of the quantities over initial 500 cycles of magnetic oscillation are discarded and then the average of these are taken over the next 500 cycles of magnetic oscillation. Total length of simulation is 100000 MCSS. Increase in the value of order parameter below a certain temperature marks the dynamic phase transition between symmetric and symmetry-broken phase. This dynamic transition temperature is measured from the sharp peak or dip in the variation of $\frac{dQ}{dT}$, $V$ and $C_v$. It is clear from these variations that the dynamic transition occurs at *lower* temperatures for *higher* values of $S$ for a fixed value of frequency and magnetic field amplitude of propagating magnetic wave.

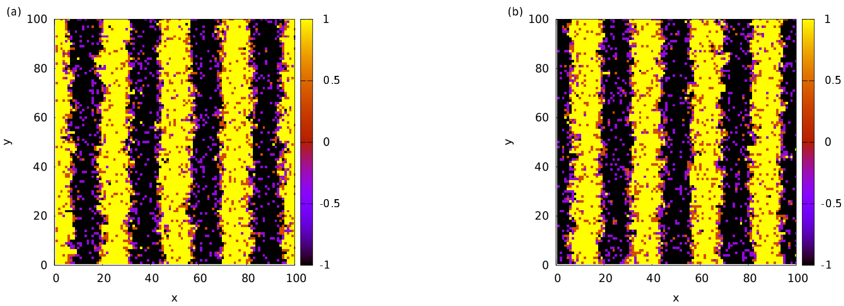


Figure 4.3: (Color online) Coherent propagation of spin-wave is shown at two different times for propagating magnetic wave: (**a**) at $t = 4018$ and (**b**) at $t = 4067$. Here $n = 4$ ($S = 3/2$), $h_0 = 1.0$ & $T = 1.2$; $f = 0.01$.

In *figure 4.3* the propagation of spin wave can be seen. *Fig.4.3(***b***)* is taken at nearly half time period later than the *fig.4.3(***a***)*. Parallel bands of spins state propagate coherently with the propagating wave. This phase is known as propagating phase. The morphology of spins in the lattice at different temperature and different values of $S$ are shown in the *figure 4.4*. These morphologies of spin structure at various temperatures in Ising ferromagnet show that there are similarities in the morphologies of spins for different $S$ values. The only difference occurs in their transition temperatures.

To know the variation of dynamic transition temperature with the value of $S$, phase boundaries are drawn in $h_0 - T_d$ plane for different values of $S$. Such a phase diagram is shown in the *figure 4.5*. The phase boundaries shrink inward (lower values of $h_0$ and $T_d$) for higher $S$ values. These phase diagrams also reveal in details that in a general spin-$S$ ferromagnet, the dynamic transition temperature *decreases* with the increase in the number of states ($n = 2S + 1$) of the spin-$S$ ferromagnet. The energy gap between

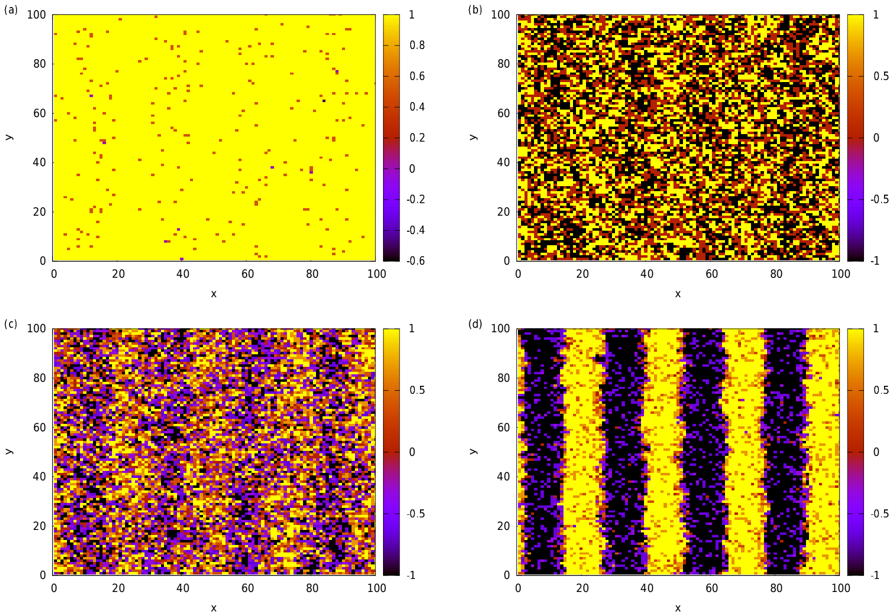


Figure 4.4: (Color online) Lattice morphology (value of $s^z(x, y, t)$) at time $t = 4000$ for different values of $n = 2S + 1$, $h_0$ and $T$ for propagating magnetic wave: (**a**) $n = 5$, $h_0 = 0.8$ & $T = 0.5$, (**b**) $n = 3$, $h_0 = 0.2$ & $T = 2.8$, (**c**) $n = 7$, $h_0 = 0.3$ & $T = 1.8$ and (**d**) $n = 7$, $h_0 = 1.2$ & $T = 0.8$.

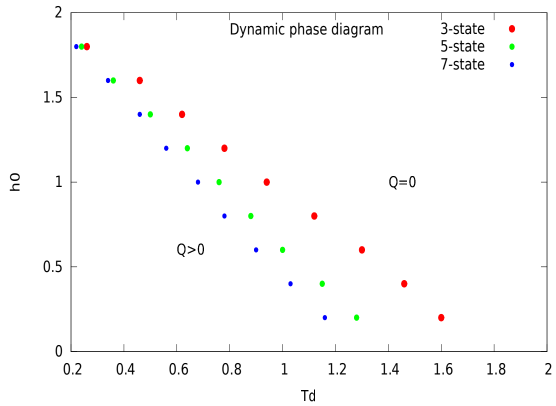


Figure 4.5: (Color online) Phase diagram in $T_d$-$h_0$ plane for *3-state* (red dot), *5-state* (green dot) and *7-state* (blue dot) spins for propagating wave.

these $n$-states is smaller for higher values of spin $S$ as compared to that for smaller values of $S$. As a result, ferromagnetic spins fluctuate between these states easily when driven by external perturbation. This leads to the symmetric distribution of the ferromagnetic spins around $s^z = 0$. Thus, the value of order parameter becomes small. Therefore, the system passes into the spin frozen phase (or symmetry-broken phase) from the symmetric phase at lower temperatures for higher values of spin $S$. This result is similar to what we have seen in *figure 4.2*. For a higher value of spin-$S$; i.e. ferromagnets having greater number of spin states, the transition temperature decreases while the magnetic field amplitude $h_0$ is kept fixed. The dynamic transition temperature is observed to decrease towards a limiting value (in the limit of very large number of states) with greater number of spin states.

Here, it may be noted that the typical size of the error bar of the data in *figure 4.2* is around 0.03. The maximum possible error in estimating the transition temperature is the value of $\Delta T$ by which the temperature of the system is decreased. This value equals to 0.02. Thus, this is the estimate of the error in transition temperature.

### 4.2.2 Response to standing magnetic wave:

I will now discuss the effect of standing magnetic wave on general spin-$S$ Ising ferromagnet. The Hamiltonian for the Ising ferromagnet, having $(2S+1)$ numbers of spin states and uniform nearest neighbor interaction, under the influence of standing magnetic wave has the same form as *equation 5.1*, which may be rewritten here as follows:

$$H(t) = -J\Sigma\Sigma' s^z(x,y,t)s^z(x',y',t) - \Sigma h^z(x,y,t)s^z(x,y,t).$$

The magnetic wave, which keeps the system away from equilibrium is the standing magnetic field wave. The form of standing magnetic wave is–

$$h^z(x,y,t) = h_0 sin(2\pi ft) sin(2\pi\frac{x}{\lambda}).$$

Here, the parameters and variables used, have their usual meaning as mentioned in the previous *section 4.2.1*. The distribution of all the different $(2S+1)$ spin states $(s^z = +1, ..... -1)$ depends on different parameters such as temperature $T$, strength of magnetic field $h_0$ and the mutual cooperative interaction strength $J$. For simplicity $J$ is considered to be uniform throughout the system.

#### Monte-Carlo Simulation:

An $L \times L$ square lattice of Ising ferromagnetic spins is simulated to understand the dynamical phase transition under the influence of magnetic field. The spatio-temporal variation of magnetic field was considered to be in the form of standing magnetic wave. Translational invariance is kept by applying periodic boundary conditions in both the directions. The standard *Monte-Carlo* method is used to generate the dynamics of spins of the $S$-spin Ising ferromagnet. The system is cooled down slowly in steps of small change in temperature from the high temperature initial *random* configuration, to reach any dynamical state of the ferromagnet. At very high temperature, all the $(2S+1)$ spins states are equally probable. The system is brought to thermal equilibrium at any particular temperature $T$ by keeping it in that constant temperature bath for a sufficiently long time. Using MC technique, the spin dynamics may be viewed and the steady state quantities are calculated. Every spin changes its state at Metropolis rate or probability, given by *equation 2.3*;

$$W(s_i^z \rightarrow s_f^z) = Min[exp(-\Delta E/kT), 1].$$

As our usual convention the field amplitude $h_0$ is measured in the unit of $J$ and the temperature $T$ is measured in the unit of $\frac{J}{k}$. Time is measured in the unit of standard Monte-Carlo time *MCSS*. During 1 MCSS time an $L^2$ number of spins are updated once in an $L \times L$ square lattice.

**Results:**

When a $S$-spin Ising ferromagnet is kept under standing magnetic field wave the system undergoes dynamic phase transition as the temperature is cooled below a certain transition temperature. The instantaneous value of magnetization per site is expressed as: $M(t) = \frac{1}{L^2}\sum_i s_i^z(x,y,t)$. Since, $M(t)$ oscillates symmetrically about zero value ($M(t) = 0$) in the $M(t)$ $vs$ $t$ curve, the high temperature phase is called the *symmetric* phase. Whereas, in low temperature, $M(t)$ $vs$ $t$ curve is not symmetric about the $M(t) = 0$ line. This is the *symmetry-broken* or the spin-frozen phase. At very high temperature spins are randomly distributed over all the $2S+1$ spin states, corresponding to a $S$-spin system, with equal probability. Here the mutual interaction between the neighboring spins is effectively weaker than thermal fluctuations. As a result the magnetization per site $M(t)$ at any time $t$ is nearly zero. At lower temperatures (but above the transition temperature) spin-magnetic field interaction increases and the spins coherently follow the magnetic field oscillations.

*Figures 4.6(***b***)* and *4.6(***d***)* represent symmetric phase for $S = 1$ and $S = 3$ system respectively. For a lower magnetic field amplitudes and temperatures ( which are below the transition temperature) mutual interaction between any pair of spins does not allow

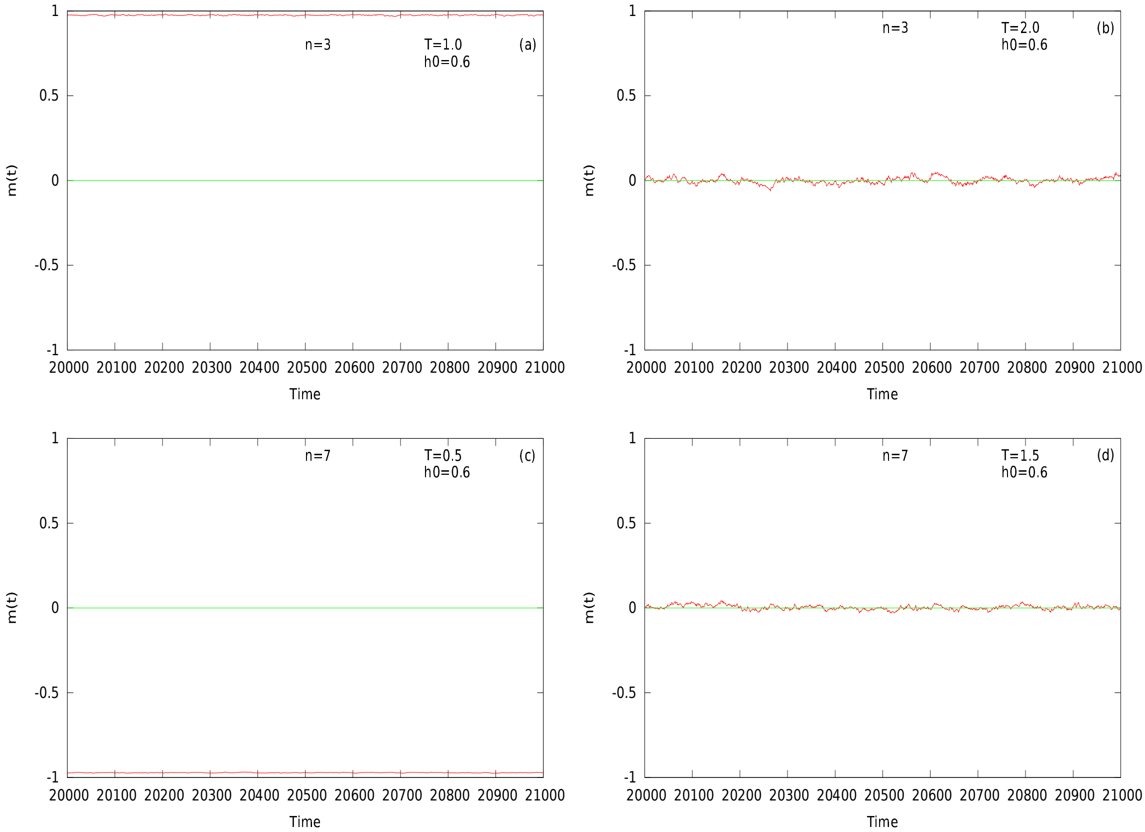


Figure 4.6: (Color online) Variation of magnetization with time at constant temperature ($T$) and field amplitude ($h_0$) for standing wave. Figs. (**a**) & (**b**) represent *3-state* spin ($S = 1$) whereas figs. (**c**) & (**d**) represent *7-state* spin ($S = 3$). Frequency $f = 0.01$.

them to follow the magnetic field variations and these spins are locked in a particular direction giving rise to a non-zero value of magnetization as shown in the *figures 4.6(***a***)* and *4.6(***c***)* for $S = 1$ and $S = 3$ spin ferromagnet respectively. Unlike in propagating magnetic field wave, in standing magnetic wave there is a local variation of field amplitude; zero at the nodes and maximum at the anti-nodes. Therefore, at nodes of the standing magnetic wave, the dynamics of the spin states are always thermally driven. But at the anti-nodes the value of field amplitude strongly affect the spin flip above the transition temperature. Above the transition temperature alternate spin bands ($s^z = +1 \; or \; -1$) form standing wave of spins, unlike the case of propagating magnetic wave. Notice that these are not the conventional spin waves in ferromagnetic materials.

The order parameter $Q$ is defined in the usual way, as described in the previous sections. It is seen that the order parameter $Q$ increases continuously from zero (nearly) to nonzero value below transition temperature. This marks the dynamical phase transition.

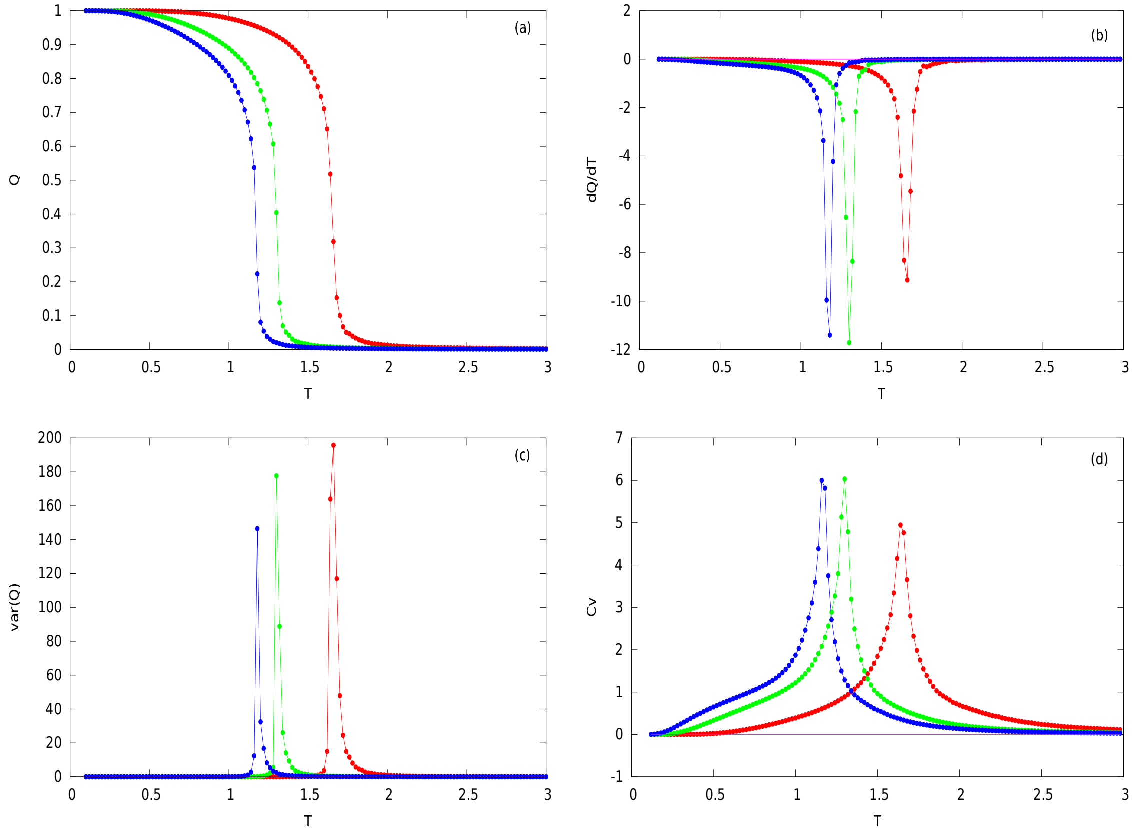


Figure 4.7: (Color online) Temperature variation of (**a**) $Q$, (**b**) $\frac{dQ}{dT}$, (**c**) $V$, (**d**) $C_v$ for *3-state* (red dot), *5-state* (green dot) and *7-state* (blue dot) spins for constant field amplitude ($h_0 = 0.2$) and frequency ($f = 0.01$) of standing wave.

The transition temperature is detected from the peaks (or dip) in the steady state temperature variations of $\frac{dQ}{dT}$, $V$ and $C_v$ near the transition temperature. These variations are shown in the *figure 4.7*. We observe that the transition temperature decreases as the number of spin states increases.

The qualitative nature of phase transition of a $S$-spin Ising ferromagnet under propagating magnetic field wave as well as standing magnetic field wave is same but the morphologies of the spins at different times in symmetric disordered phase are quite different. Unlike in propagating magnetic wave, there is no coherent propagation of spin-bands in standing magnetic wave. Instead, the alternate spin bands oscillate out of phase. This is shown in the *figure 4.8*. *Fig.4.8(***b***)* is taken at nearly quarter time period later than the *fig.4.8(***a***)*. This phase is also known as *oscillating spin clusters* phase. *Figure 4.9* show the morphological structure of $S$-spin Ising ferromagnet at different temperatures, field amplitudes and for different values of $S$.

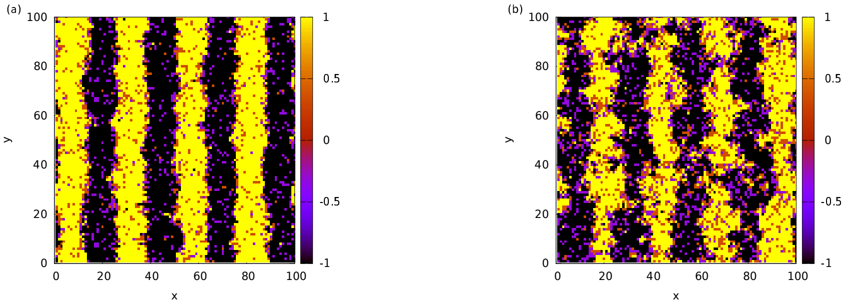


Figure 4.8: (Color online) Morphologies of standing wave dynamical modes (non-propagating) for standing magnetic wave are shown at two different times: (**a**) at $t = 4040$ and (**b**) at $t = 4067$. Here $n = 4$ ($S = 3/2$), $h_0 = 1.2$ & $T = 1.2$; $f = 0.01$.

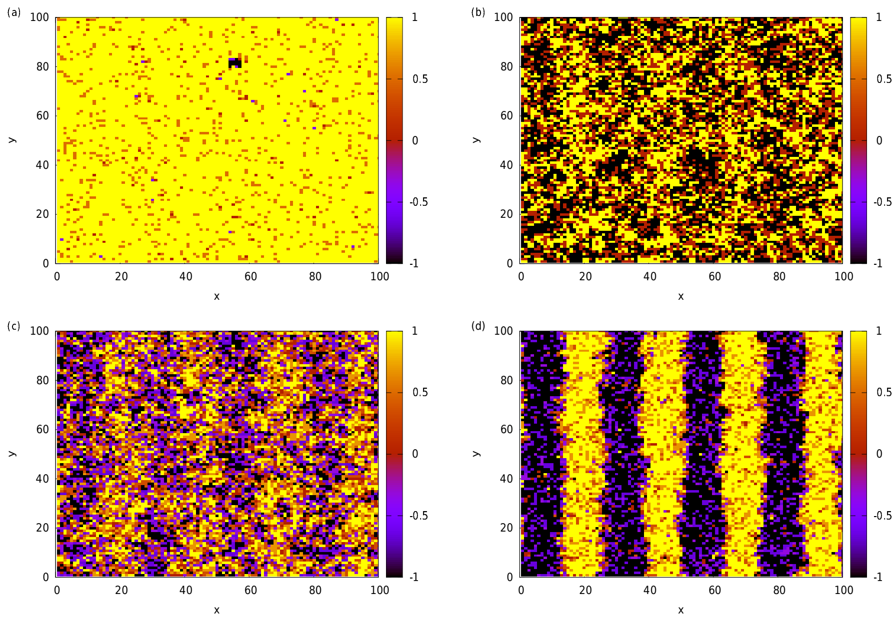


Figure 4.9: (Color online) Lattice morphology (value of $S^z(x, y, t)$) at time $t = 4000$ for different values of $n = 2S + 1$, $h_0$ and $T$ for standing magnetic wave: (**a**) $n = 5$, $h_0 = 0.8$ & $T = 0.8$, (**b**) $n = 3$, $h_0 = 0.2$ & $T = 2.2$, (**c**) $n = 7$, $h_0 = 0.3$ & $T = 1.5$ and (**d**) $n = 7$, $h_0 = 1.2$ & $T = 1.0$.

The phase boundaries drawn in the $h_0 - T_d$ plane (see *figure 4.10*) shrink inward for greater $S$ values. The data used in all the figures here are obtained for a typical $100 \times 100$ square Ising lattice. The frequency ($f$) and the wavelength ($\lambda$) of the standing wave are respectively 0.01 $MCSS^{-1}$ and 24.5 $lu$. So, the magnetic field oscillates exactly in 8 loops in a lattice. At each temperature, the system is allowed to pass through 2000 complete cycles (or 200000 MCSS) of magnetic field oscillation (in time). Steady-state behavior of dynamical quantities are measured after discarding initial 50% data and then averaging over the rest data for 100000 MCSS. The typical size of the error bar is same as in the case of propagating magnetic wave.

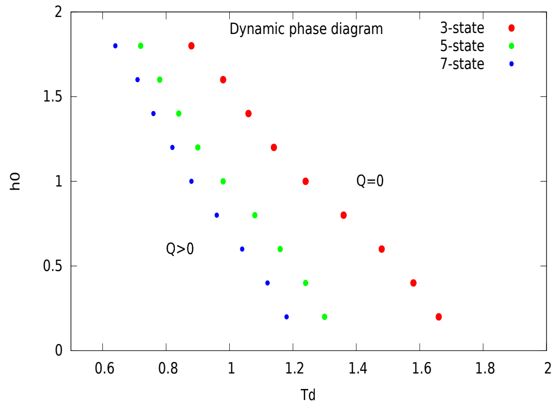


Figure 4.10: (Color online) Phase diagram in $T_d$-$h_0$ plane for *3-state* (red dot), *5-state* (green dot) and *7-state* (blue dot) spins for standing wave.

### 4.2.3 Response to magnetic field; uniform over the space but oscillating in time:

The dynamical response of a two dimensional Ising (spin-$\frac{1}{2}$) ferromagnet to an oscillating (in time but uniform over space) magnetic field has been studied earlier [1] in details. These studies reveal the hysteretic behavior and the nonequilibrium phase transition in such system. Mainly, the frequency and field dependencies of their dynamical responses, the nature of phase transition, stochastic resonance and the appropriate scaling form are studied in such ferromagnetic systems. However, the dynamical response of general spin-$S$ Ising ferromagnet under the influence of uniformly oscillating magnetic field was not studied earlier. This study is presented here in details. The Hamiltonian for the $S$-spin Ising ferromagnet under the influence of uniformly oscillating magnetic field has the same form as *equation 5.1*, which is rewritten here as follows:

$$H(t) = -J\Sigma\Sigma' s^z(x,y,t)s^z(x',y',t) - \Sigma h^z(x,y,t)s^z(x,y,t).$$

The standard form of uniformly oscillating magnetic field (having no spatial variation) is given by:

$$h^z(x,y,t) = h_0 cos(2\pi ft).$$

Here, the parameters and variables used, have their usual meaning as mentioned in the previous *section 4.2.1*. $J$ is uniform all over the lattice and interaction between spins is present up to the nearest neighbors. "$\Sigma'$" indicates that summation is extended up to nearest neighbors only. Ferromagnetic spins are distributed over $2S+1$ numbers of spin states depending upon the values of temperature $T$ and magnetic field amplitude $h_0$ for a particular value of $S$.

**Monte-Carlo Simulation:**

Here also, the standard Monte-Carlo method is applied to simulate the dynamical responses in the ferromagnet. With periodic boundary conditions applied in both directions of an $L \times L$ square lattice, the ferromagnetic spins are updated at Metropolis rate given by the *equation:2.3*

$$W(s_i^z \to s_f^z) = Min[exp(-\Delta E/kT), 1].$$

$s_i^z$ and $s_f^z$ are respectively, the initial and final values of any spin state at a site $(x, y)$, before and after updating. $\Delta E$ represents the change in energy due to spin flip from initial state to final state; $k$ is the Boltzmann constant. The units of field amplitude $h_0$ and temperature $T$ are respectively $J$ and $\frac{J}{k}$. The unit of time is *MCSS*. Starting from initial high temperature configuration the system is cooled slowly in small steps of temperature. The system is allowed to be in contact with a heat bath, having a fixed temperature for a sufficiently long time so that nonequilibrium steady state is reached.

**Results:**

Under uniformly oscillating magnetic field also, two distinct phases, namely: high temperature *symmetric* phase and low temperature *symmetry broken* phase are observed. At sufficiently high temperature spins are uniformly distributed over all of its $2S+1$ states. In the high temperature, due to small intrinsic relaxation time, the system follows the magnetic field. As a result, magnetization $M(t)$ coherently and symmetrically oscillates around zero value (of magnetization) and the order parameter $Q$ becomes nearly zero. This phase is called the *uniformly oscillating* phase. The variation of magnetization with time in this phase is shown in the *figures 4.11(***b***)* and *4.11(***d***)* respectively for $S = 1$ and $S = 3$ values of Ising spins.

As the temperature is further cooled the system lags behind the magnetization variation. As a result the magnetization varies asymmetrically about zero line (of magnetiza-

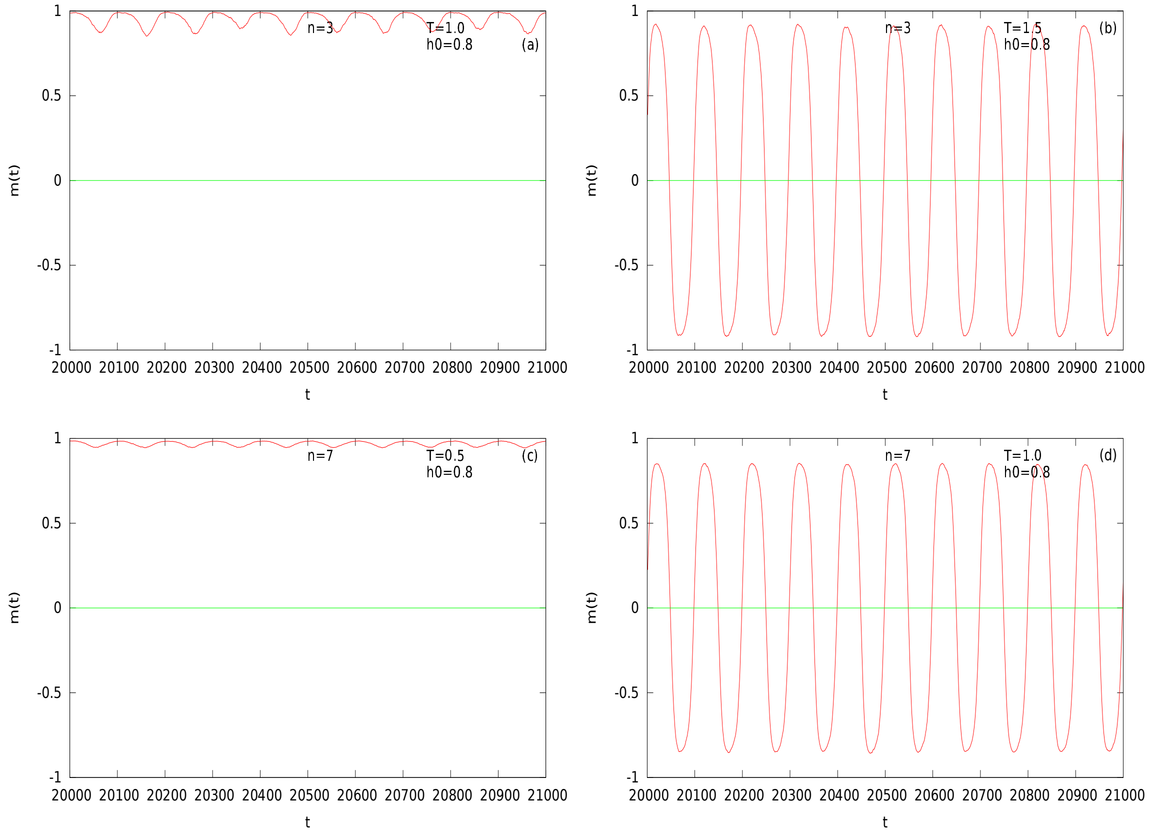


Figure 4.11: (Color online) Variation of magnetization with time at constant temperature ($T$) and field amplitude ($h_0$) for uniformly varying field. Figs. (**a**) & (**b**) represent *3-state* spin ($S = 1$) whereas figs. (**c**) & (**d**) represent *7-state* spin ($S = 3$). Frequency $f = 0.01$.

tion). This gives rise to a phase transition from high temperature symmetric disordered phase to a low temperature symmetry-broken ordered phase. At very low temperatures, which are below the transition temperature most of the spins orient in a single direction and the net magnetization grows, which is shown in the *figures 4.11(**a**)* and *4.11(**c**)*. This phase is also called the *pinned* phase.

The value of the order parameter continuously grow from nearly zero value in symmetric phase to a nonzero value in pinned phase below certain dynamical transition temperature. The transition temperature is detected from the peaks (or dip) in the thermal variations of the quantities $\frac{dQ}{dT}$, $var\ Q$ and $C_v$ in steady state conditions. Such temperature variations are shown for three different values of $S$ in the *figure 4.12*. It is observed here also from these figures that the dynamic transition temperature decreases with the increase in the value of $S$. For higher values of spin $S$ the number of states $(2S + 1)$ of $s^z$ is also large. This enables the system to have several $s^z$ state in response

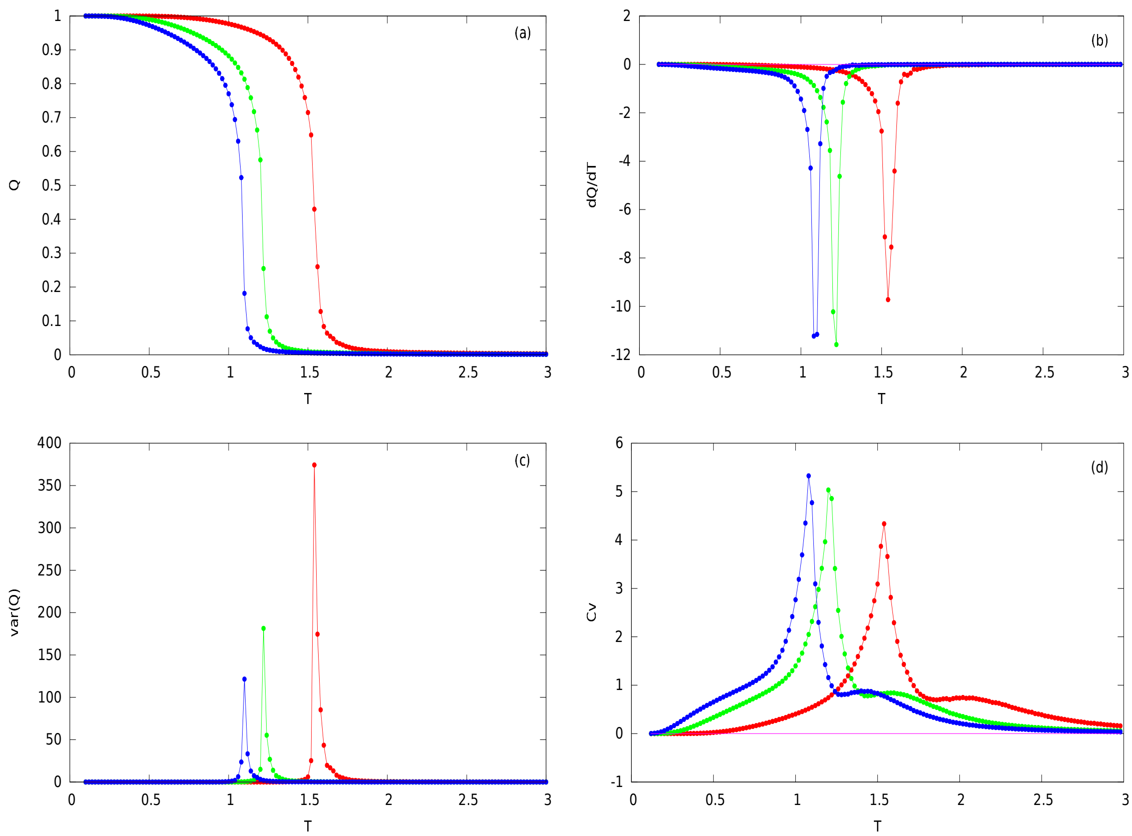


Figure 4.12: (Color online) Temperature variation of (**a**) $Q$, (**b**) $\frac{dQ}{dT}$, (**c**) $V$, (**d**) $C_v$ for *3-state* (red dot), *5-state* (green dot) and *7-state* (blue dot) spins for constant field amplitude ($h_0 = 0.3$) and frequency ($f = 0.01$) of uniformly varying field.

to the magnetic field variation. So, for a fixed temperature ($T$) and field amplitude ($h_0$) the value of the order parameter is less than that for lower value of $S$. This is the main reason to have ordering of higher $S$ at lower temperatures. The transition temperature are much closer for higher values of $S$ and it approaches a limiting value in the limit of very large value of $S$.

The morphology of spins in uniformly oscillating phase is shown at two different times in *figure 4.13*. These snapshots show the difference of the morphological structures of spins within the lattice under uniformly (over the space) oscillating field with those of the propagating wave and standing wave. Since there is no spacial variation of magnetic field we cannot observe any significant pattern of spins here.

The spin configurations for different $T$, $h_0$ and $S$ are shown in the *figure 4.14*. The phase boundaries may also be drawn for different values of $S$ in the plane of $h_0$-$T_d$. These phase boundaries shrink inward (lower values of $h_0$ and $T_d$) for higher values of $S$ and

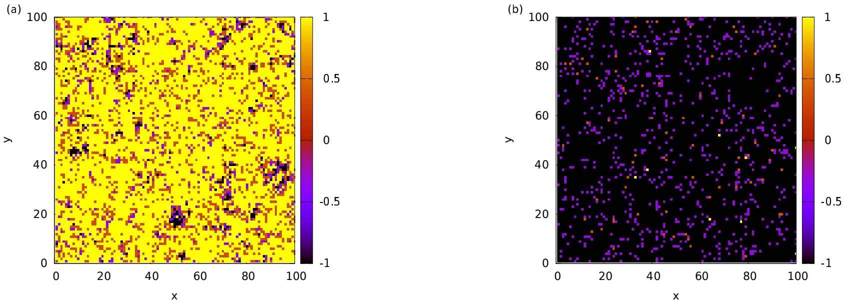


Figure 4.13: (Color online) Oscillation of spins shown at different times ($t = 4000$ & $t = 4067$) in symmetric phase for uniformly oscillating magnetic field. Here $n = 4$ ($S = 3/2$), $h_0 = 1.2$ & $T = 1.2$; $f = 0.01$.

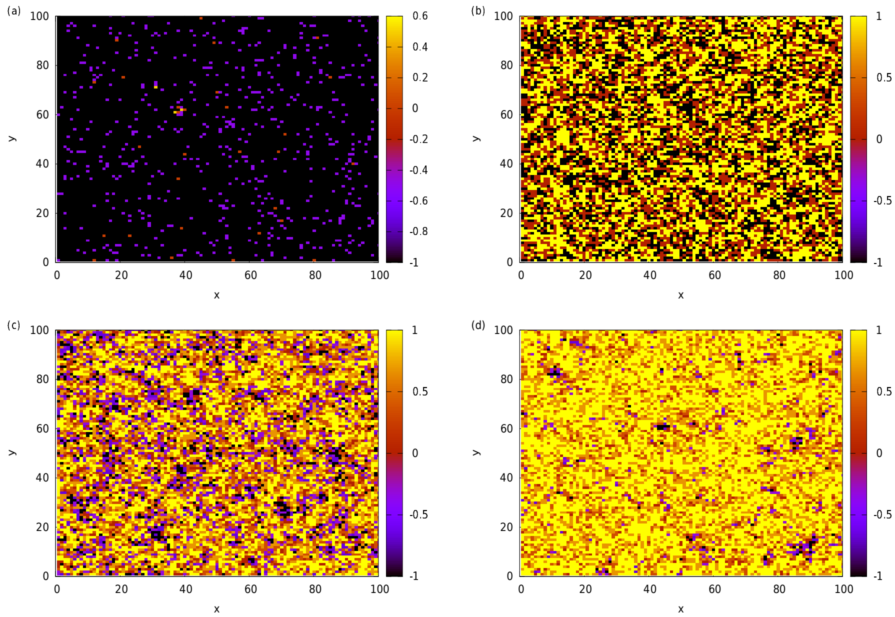


Figure 4.14: (Color online) Lattice morphology (value of $S^z(x, y, t)$) for different values of $n = 2S+1$, $h_0$ and $T$ for uniformly oscillating magnetic field: (**a**) $n = 5$, $h_0 = 0.8$ & $T = 0.8$ at time $t = 3950$ and (**b**) $n = 3$, $h_0 = 0.2$ & $T = 2.9$, (**c**) $n = 7$, $h_0 = 0.3$ & $T = 1.5$, & (**d**) $n = 7$, $h_0 = 1.2$ & $T = 1.0$ at time $t = 4000$.

appear to converge on a limiting value in the limit of very high value of $S$ for which each spin can take practically any value between $+1$ and $-1$ in the limit $S \rightarrow \infty$.

Thus, all the studies described in the *sections 4.2.1, 4.2.2 and 4.2.3* reveal that the nature of dynamic phase transition under different kind of magnetic field perturbation is qualitatively same in a gross picture. This is the main observation here. But, there exist significant differences in the morphological patterns and dynamics of spins in both kind of phases, specially in the high temperature phases, formed under the influence of different kind of magnetic field variations. These differences are due to the nature

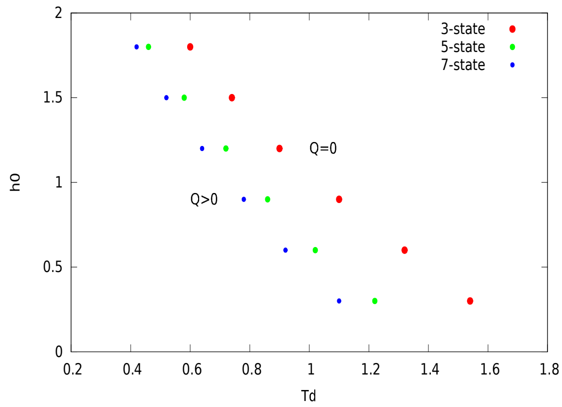


Figure 4.15: (Color online) Phase diagram in $T_d$-$h_0$ plane for *3-state* (red dot), *5-state* (green dot) and *7-state* (blue dot) spins for uniformly varying field.

of spatio-temporal variations present in the magnetic field that influences the system externally.

The studies, discussed so far, find motivation with experimental background. Using meanfield renormalization group analysis, the site diluted Blume-Capel model was studied [19]. The results were in good agreement with the experimental phase diagram of **Fe-Al** alloy. In the studies presented here , this may be generalized for $S = 1$ Ising ferromagnet. Using time resolved magneto optic Kerr (TRMOKE) effect this kind of coherent propagation of spin bands and other dynamical patterns of spin waves may be experimentally studied. I believe, that this has a significant role in the field of spintronics and magnonics [20]. The magnetic behaviors of core-shell magnetic nanoparticles have important implications in the magnetism research as well as in the technology. In bi-magnetic ($FePt/MFe_2O_4(M = Fe, Co)$) core-shell nanoparticles also, the properties of magnetism have been studied [21] . The nonequilibrium phase transition has been studied [22] by Monte Carlo simulation in spherical core-shell ($S = 3/2$ core and $S = 1$ shell) magnetic nanoparticles under *time dependent* (uniform over space) magnetic field. In the view of such experimental success, I propose for an experimental study of the dynamic responses of core-shell magnetic nanoparticles in the presence of magnetic field having spatio-temporal variation in the form of propagating and standing magnetic wave.

## Bibliography:


1. B. K. Chakrabarti and M. Acharyya, *Rev. Mod. Phys.* **71** (1999) 847;
   M. Acharyya, *Int. J. Mod. Phys. C* **16** (2005) 1631.
2. M. Acharyya, *Int. J. Mod. Phys. C* **14** (2003) 49.
3. H. Jung, M. J. Grimson, C. K. Hall, *Phys. Rev. B* **67** (2003) 094411
   H. Jung, M. J. Grimson, C. K. Hall, *Phys. Rev. E* **68** (2003) 046115.
4. M. Keskin, O. Canko, B. Deviren, *Phys. Rev. E* **74** (2006) 011110.
5. M. Ertas, B. Deviren and M. Keskin, *Phys. Rev. E*, **86** (2012) 051110.
6. U. Temizer, *J. Magn. Magn. Mater*, **372** (2014) 47.
7. E. Vatansever, A. Akinci and H. Polat, *J. Magn. Magn. Mater*, **389** (2015) 40.
8. M. Ertas and M. Keskin, *Physica A*, **437** (2015) 430.
9. X. Shi, L. Wang, J. Zhao, X. Xu, *J. Magn. Magn. Mater*, **410** (2016) 181.
10. D. M. Saul, M. Wortis and D. Stauffer, *Phys. Rev. B*, **9** (1974) 4964.
11. A. K. Jain and D. P. Landau, *Phys. Rev. B*, **22** (1980) 445.
12. M. Deserno, *Phys. Rev. E*, **56** (1997) 5204.
13. J. C. Xavier, F. C. Alcaraz, D. P. Lara, J. A. Plascak, *Phys. Rev. E*, **57** (1998) 11575.
14. M. Ertas, M. Keskin and B. Deviren, *J. Magn. Magn. Mater*, **324** (2012) 1503.
15. M. Acharyya, *Acta Physica Polonica B*, **45** (2014) 1027.
16. A. Halder and M. Acharyya, *J. Magn. Magn. Mater*, **420** (2016) 290.
17. M. Acharyya and A. Halder, *J. Magn. Magn. Mater*, **426** (2017) 53.
18. K. Binder and D. W. Heermann, Monte Carlo simulation in statistical physics, Springer series in solid state sciences, Springer, New-York, 1997.
19. D. Das and J. A. Plascak, *Phys. Lett. A*, **375** (2011) 2089.
20. S. Bader and S. S. P. Parkin, *Annu. Rev. Condens. Matter Phys*, **1** (2010) 71-88.
21. H. Zeng, S. Sun, J. Li, Z. L. Wang and J. P. Liu, *Applied Physics Letters*, **85** (2004) 792.
22. E. Vatansever and H. Polat, *J. Magn. Magn. Mater*, **343** (2013) 221.